Modelling rutile TiO 2 nanorod growth preferences: a Density Functional Theory study

Hsin-Hung Chou, Sofia Ya-Hsuan Liou, Monica Calatayud

Modelling rutile TiO_2 nanorod growth preferences: a Density Functional Theory study

Hsin-Hung Chou[1,2], Sofia Ya-Hsuan Liou[2,*], Monica Calatayud[1,*]

[1] Sorbonne Université, CNRS, Laboratoire de Chimie Théorique, LCT, F. 75005 Paris, France

[2] Department of Geosciences and NTU Research Center for Future Earth National Taiwan University

*corresponding authors:

M. Calatayud

calatayu@lct.jussieu.fr

Laboratoire de Chimie Théorique

Sorbonne Université

4, Place Jussieu case 137 Paris-France

Phone : +33 1 44 27 41 17

Fax : +33 1 44 27 41 17

S. Y. H. Liou

yhliou@ntu.edu.tw

Phone : +886 233669861

Environment and Nanomaterial Lab

Department of Geosciences, National Taiwan University

No. 1, Sec. 4, Roosevelt Road, Taipei 106, Taiwan

Abstract

Synthesis of 1D TiO_2 nanorods is promising nowadays owing to their broad applications in photocatalytic devices. A groundbreaking synthesis procedure of one-step producing large-scale, free-standing and heterogeneous phase (anatase and rutile) 1D TiO_2 nanorod array which efficiently enhances the photocatalytic activity has been previously proposed. However, the detailed growth mechanism of this catalyst remains unclear, mainly because the synthesis takes place in a closed autoclave.

This study presents a complementary approach to understand the growth mechanism using computer modeling based on density functional theory (DFT). The interaction of the precursor (titanium butoxide in hydrochloric acid media, modelled by $TiCl_4$) and solvent (water) with preexisting rutile titania is computed to derive the thermodynamic trends to grow additional TiO_2 layers. Five different termination models of the rutile's surfaces were built: (001), (100), (101), (110) and (111), and their interaction with precursor and water was computed. Molecular and dissociative adsorption are considered as well as coadsorption. Our results point to a preferential growth of the (001) termination of rutile TiO_2 through intermediates involving $TiCl_3^+$, Cl^- and hydroxyl groups. The results obtained show how computational chemistry can be used to resolve experimental growth information. The protocol used i.e. computing different terminations and their explicit interaction with both the precursor and the solvent, can be extended to other materials in which the growth takes place following well-defined preferential directions.

Keywords: mixed phase、TiO_2、nanorods、surface energy、Density Functional Theory

1. Introduction

One dimensional (1D) TiO_2 nanorod is declared as an effective, stable and nontoxic photocatalyst widely employed in technological applications[1]. Various studies have focused on the improvement of this photocatalytic material. The mixture of anatase and rutile of TiO_2 has proven to enhance the spatial charge separation and hinder recombination across the phase interfaces[2]. One-step synthesis of free-standing geometry is desired since it may extend the range of applications, increase the photocatalytic activity and avoid structural destruction. A groundbreaking method [3] has been developed to achieve those advantages. The method consists of a thermal system including transparent conductive fluorine-doped tin oxide (FTO) substrates, titanium butoxide precursor (TBOT), concentrated hydrochloric acid (HCl) and Ti foil which subsequently transforms to $TiCl_4$ in a Teflon-lined stainless steel autoclave. A large-scale and free-standing 1D mixed phase TiO_2 nanorod array film is successfully obtained. Kao et al. [3]demonstrate the sequence growth of rutile and anatase TiO_2 in the synthesis process. The anatase TiO_2 grows based on the existence of rutile TiO_2, that is controlled by the duration of the synthetic procedure and grows in the (001) direction. The detailed growth mechanism during the thermal reaction remains unclear, in particular the role of the Ti and O precursors in the preferential orientation of the nanorod, and motivates the present work.

The difficulty of resolving the detailed mechanism from a closed, high temperature and pressure synthesis system (autoclave in an oven) is insurmountable. *Ab initio* modeling may be a suitable alternative since it provides a molecular view of the interactions between titania and its environment. Density Functional Theory (DFT) is a robust approach successfully used to treat titania-based materials with an excellent accuracy-cost ratio. The literature on modelling rutile bulk[2d, 4], surface[5], nanoparticles [6]and nanoclusters[7] is abundant and shows that the method is reliable as regards geometry and energetics, whereas accurate electronic structure features need specific approaches. The aim of the present study is to provide an atomic picture of the interaction of rutile with its environment that may occur during the thermal synthesis of titania nanorods, bringing insight in the growth mechanism. Focus will be put on the thermodynamic aspects governing the process i.e. energetics of the adsorption of Ti- and O-precursors on different rutile terminations, so as to identify preferential interactions that guide the growth. The paper is organized as follows. Section 2 describes the computational protocol and the models used. Section 3 presents and discusses the results obtained as regards the interaction of water and precursor model $TiCl_4$ with the TiO_2 terminations, and their coadsorption. Finally, the

conclusions raised are summarized.

2. Computational details

2.1. Methods

Our calculations were performed within the Density Functional Theory as implemented in the Vienna Ab initio Simulation Package (VASP) – version 5.4.1[8]. Generalized Gradient Approximation (GGA) was applied for exchange and correlation potential with the Perdew-Becke-Ernzerhof (PBE) functional[9]. According to the Projector Augmented Wave (PAW) method[10], core electrons were frozen and replaced by pseudopotentials (Ti, O_s, H, Cl_s). The valence electrons (Ti: $4s^2 3d^2$; O: $2s^2 2p^4$; H: $1s^1$; Cl: $3s^2 3p^5$) were expanded in a plane wave basis set with kinetic energy cutoff of 300 eV. The Brillouin zone was sampled using the Monkhorst-Pack scheme with automatic k-points mesh generation for structural optimizations, spaced ~0.04 $Å^{-1}$. Geometrical optimization is performed by means of the conjugate-gradient algorithm (treshold 0.1 meV in the total energy). All atoms are allowed to relax.

2.2. Slab models

The slab models were constructed from the bulk tetragonal rutile lattice a = b = 4.594 Å, c = 2.958 Å, u = 0.305. Its space group is $P4_2$ / mnm and the cell contains 2 TiO_2 units. Ti atoms are six-fold coordinate and oxygen atoms are three-fold coordinate.

The slab models were built with the MAPS program (Scienomics) by orienting the bulk in the low-index Miller directions [110], [001], [100], [101] and [111] as in Figure 1. A vacuum of at least 15 Å is used to avoid interaction between successive slabs.The slabs were terminated by cutting the least number of bonds with respect to the bulk, and 2x2 units were employed. The slabs used are available in supplementary material. The surface energy of the five slabs used was calculated following Eq. 1:

Eq. 1. $$E_{Surface} = \frac{E_{Slab} - N \cdot E_{Bulk}}{2A}$$

where E_{Slab} is the total energy of the slab, E_{Bulk} is the total energy of bulk, N is the number of bulk units in the slab, and A is the surface area. Stoichiometric compositions were considered.

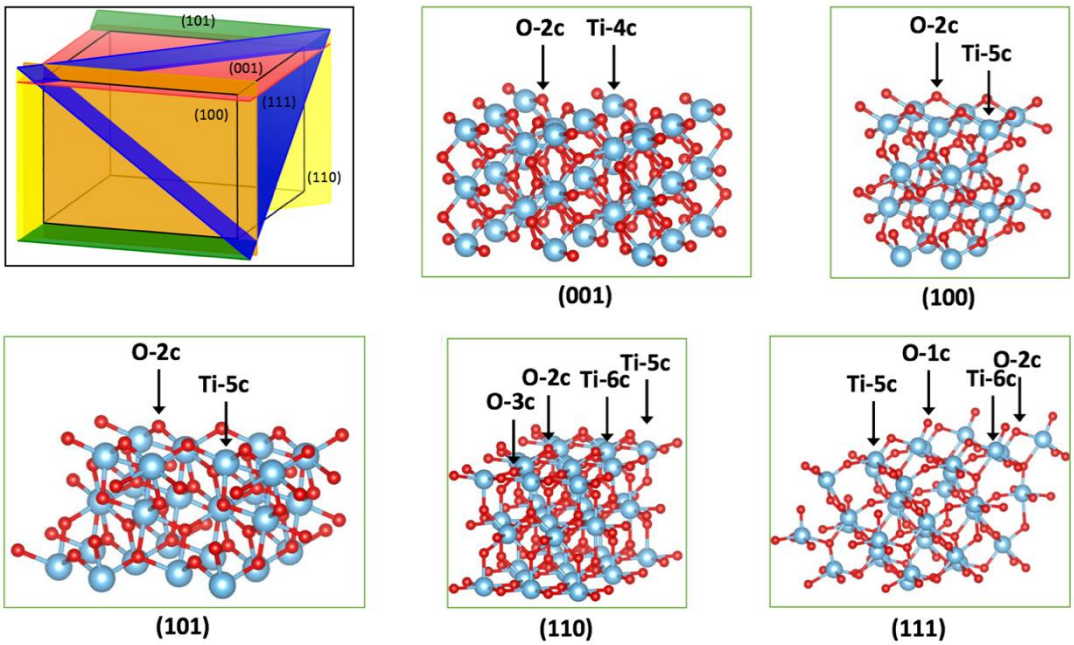

Figure 1. Representation in perspective of the (001), (101), (110), (100) and (111) surfaces with coordination number of atoms at the surface where Ti-nc and O-nc are titanium and oxygen of coordination number n. Titanium cations are represented in light blue and oxygen anions in red.

2.3. Adsorption of H_2O and $TiCl_4$

We focus on these molecules because they play an essential role in the system of the 1D mixed phase TiO_2 nanorod growth model. H_2O is considered as the source of oxygen and is present in large excess as solvent. $TiCl_4$ is considered as the source of titanium. Actually, the precursor introduced in the autoclave is TBOT, which presumably transforms into $TiCl_4$ under reaction conditions of temperature and pressure as described above. In the present study we consider the adsorption of each molecule separately, and their coadsorption, on the five different slabs, so as to characterize the energetic and structural features that could explain the preferential growth in the [001] direction. The adsorption systems were modeled on those five stoichiometric surfaces of rutile TiO_2 by adding the molecules to one side of the slab. Figure 2 schematizes the adsorption modes explored in this work.

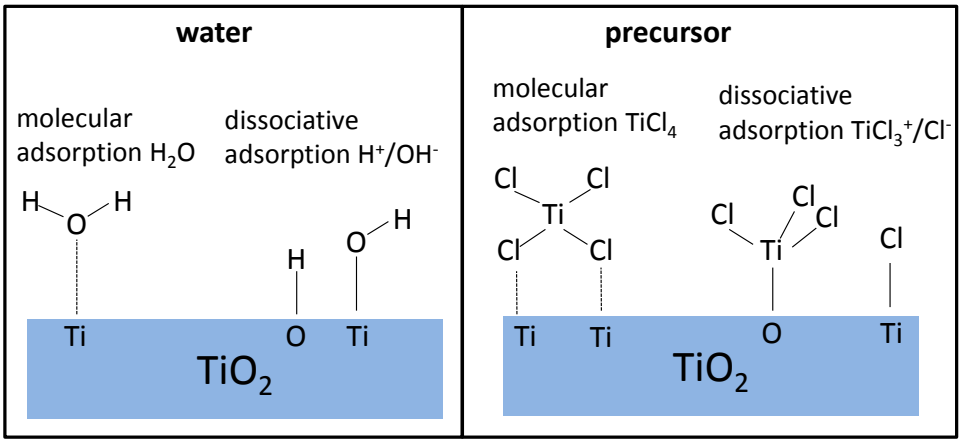

Figure 2: scheme of the adsorption modes considered in the present work for water and precursor $TiCl_4$.

The adsorption energy for a molecule is defined as the difference between the energy of the adsorption system $E_{surface+adsorbate}$ and the sum of the energy of the surface and the adsorbate in gas-phase $E_{surface} + E_{adsorbate}$:

Eq. 2. $E_{ads} = E_{surface+adsorbate} - (E_{surface} + E_{adsorbate})$

The gas-phase adsorbates ($TiCl_4$ or water) were calculated in a box of dimensions 20x20x20 $Å^3$.The lower (negative) the adsorption energy, the more stable the adsorption system. The coadsorption systems are described in more detail in section 3.4.

3. Results

3.1. Bare slabs

The surface energy of each stoichiometric surface of rutile TiO_2 was calculated following Eq. 1 and the calculated values are displayed in Table 1. The lowest surface energy is found for the (110) slab, 0.48 Jm^{-2}, followed by (100) with 0.68 Jm^{-2}, (101) 0.96 Jm^{-2}, (001) 1.28 Jm^{-2} and (111) 1.45 J m^{-2}. The results are fully consistent with the literature[5d, 11]and confirm the high thermodynamic stability of the (110) termination.

Table 1. The calculated surface energy ($J \cdot m^{-2}$) for the five terminations considered.

Surfaces	(001)	(100)	(101)	(110)	(111)
This study	1.28	0.68	0.96	0.48	1.45
Hardcastle et al.[11]	1.15	0.62	0.98	0.42	1.33
Perron et al. [5d]	1.21	0.67	1.01	0.48	-

3.2. Adsorption of water

The adsorption energies of H_2O on the five stoichiometric surfaces of rutile TiO_2 were calculated in two steps. First, one H_2O was added to the slab (1^{st} H_2O), exploring the different adsorption sites and considering both molecular and dissociative modes. Three initial orientations (upward, parallel, and downward) were tested for the molecular adsorption mode. In most of the cases the water molecule interacts with a surface under-coordinated Ti site by its oxygen site, the hydrogen atoms rearrange to maximize hydrogen bonds with the substrate and neighboring molecules. The (111) termination is a particular case because it possesses one-fold coordinated oxygen that blocks the titanium site making it unavailable for interacting with H_2O. In addition, the (111) unit cell is asymmetric, here we considered two orientations (along short-axis and long-axis) in both molecular and dissociative modes. Table S1 shows the optimized structures obtained for the systems.

The adsorption energy was calculated based on Eq. 2 and is displayed in Table 2. The lowest adsorption energy (most exothermic) of each interaction type (molecular and dissociative) indicates the most favorable interaction, and the results are compared among the different terminations studied. The most exothermic adsorption energies are plotted in Fig. 3. The adsorption of a water molecule (1^{st} H_2O) results in energies ranging from -0.33 eV to -0.68 eV in the molecular form, and -0.41eV to -1.03 eV for the dissociated form. The (001) termination exhibits the most exothermic value, -1.03 eV, that corresponds to the dissociative adsorption, followed by the (111) termination with -0.78 eV also for the dissociative mode. The three other terminations show weaker interactions: (101) -0.69 eV (dissociative), (110) -0.59 eV (molecular), (100) -0.41 eV (dissociative). The dissociative mode is clearly preferred on three of the terminations i.e. (001), (101) and (111) whereas the (110) and (100) terminations show similar energies for molecular and dissociative modes. It can be observed in Table S1 that the molecular adsorption of one water molecule leads to different geometries depending on the termination. In most of the cases the molecule connects via H-bonds to the substrate. Also the dissociative mode shows specific orientations of the surface hydroxyl groups that maximize interactions between them and with the

surface.

In order to include the effect of a higher coverage in water, which models the presence of the solvent in the experiment and acts as source of oxygen in the growth mechanism, we have considered the adsorption of a second water molecule (2^{nd}-H_2O) in the systems optimized with one molecule. The consecutive adsorption energy is calculated as in eq. 3.

Eq. 3. $E_{adsorption} = E_{surface + two-water} - (E_{surface + one-water} + E_{water})$

The geometry of the second molecule is chosen among the stable geometries of the first one i.e. in similar adsorption sites available (in the 2x2 unit cells there are 4 Ti sites available and each molecule would occupy one). The results shown in Table 2, Fig 3 indicate that the second water molecule adsorbs preferentially in the molecular mode, with the exception of the (001) termination. The range in energy goes from -0.16 eV to -1.28 eV. The adsorption of the second molecule is exothermic for all the systems, with two different behaviors. In a first group, a decrease in the strength from passing from one to two molecules is found for (001) -1.03 eV (1^{st}-H_2O) and -0.82 eV (2^{nd}-H_2O), and to a less extent for (111) -0.78 eV (1^{st}-H_2O) -0.70 eV (2^{nd}-H_2O), with water dissociated in the two steps. In a second group, the adsorption of the second water molecule becomes more exothermic than the first one for (100) -0.41 eV (1^{st} -H_2O) -0.98 eV (2^{nd}-H_2O), also observed in (101) and (110) terminations, and does not dissociate. This behavior could indicate a strong stabilization by hydrogen bonds not present in lower coverage or other terminations, that form between water-substrate and water-water. Interestingly, the (001) termination appears to be the most reactive towards water because it enables the dissociation of two water molecules: the O-H break is needed to grow TiO_2 layers from the molecules present in the reaction bath.

Our results are fully consistent with the literature[12]. The abundant data on water interaction with the most stable (110) termination point to the coexistence of dissociated and molecular water in the first monolayer, see ref. [12a, 12b] and therein. This is observed in the similar adsorption energy for the molecular and dissociated first water molecule (see ΔE_{D-M} in Table 2), which is only of -0.08 eV in favor of the latter. The same behavior is found for the (100) termination, slightly favoring the molecular adsorption. The (101) and (111) terminations show intermediate ΔE_{D-M} values of -0.12/-0.17 eV, whereas the (001) termination displays -0.35 eV in favor of the dissociative mode. Adding a second water molecule is favorable in its molecular

form for all the terminations excepted for (001), which stabilize dissociation by -0.30 eV. On a nanometric scale, the presence of surface hydroxyl groups has been found to stabilize small nanoclusters and showed adsorption energies in the range -1 to -2.5 eV depending on the coverage and the size of the nanocluster[12c]. Also, the formation of hydrogen bonds between the surface hydroxyl groups and molecular water would lead to a stabilization of the layer. Finally, the few studies on other TiO_2 terminations including rutile, anatase and brookite with water suggest a crucial role of the topology [12d-g] that we also observe in the different behavior of the five terminations considered. The ability of (001), and to a lesser extent (111) termination, to dissociate two water molecules appears as a possible factor explaining the preferential growth in those directions.

Table 2. Adsorption energy (eV) of each termination on different stoichiometric surfaces of rutile TiO_2 with one H_2O (1^{st}-H_2O) and a second water molecule on the previous most stable system (2^{nd}-H_2O). Relative energy ΔE_{D-M} corresponds to the difference between the dissociated and the molecular modes for each case. The cumulative adsorption energy is shown in the last column together with the adsorption mode (*m* for molecular, *d* for dissociative)

Surface	1^{st} H_2O			2^{nd} H_2O			1^{st}+2^{nd} H_2O
	Molecular	Dissociative	ΔE_{D-M}	Molecular	Dissociative	ΔE_{D-M}	
(001)	-0.68	-1.03	-0.35	-0.52	-0.82	-0.30	-1.85dd
(100)	-0.33	-0.41	-0.08	-0.98	-0.16	0.86	-1.39dm
(101)	-0.52	-0.69	-0.17	-1.28	-0.59	0.69	-1.97dm
(110)	-0.59	-0.51	0.08	-0.86	-0.56	0.30	-1.45mm
(111)	-0.66	-0.78	-0.12	-0.70	-0.70	0.00	-1.48dd

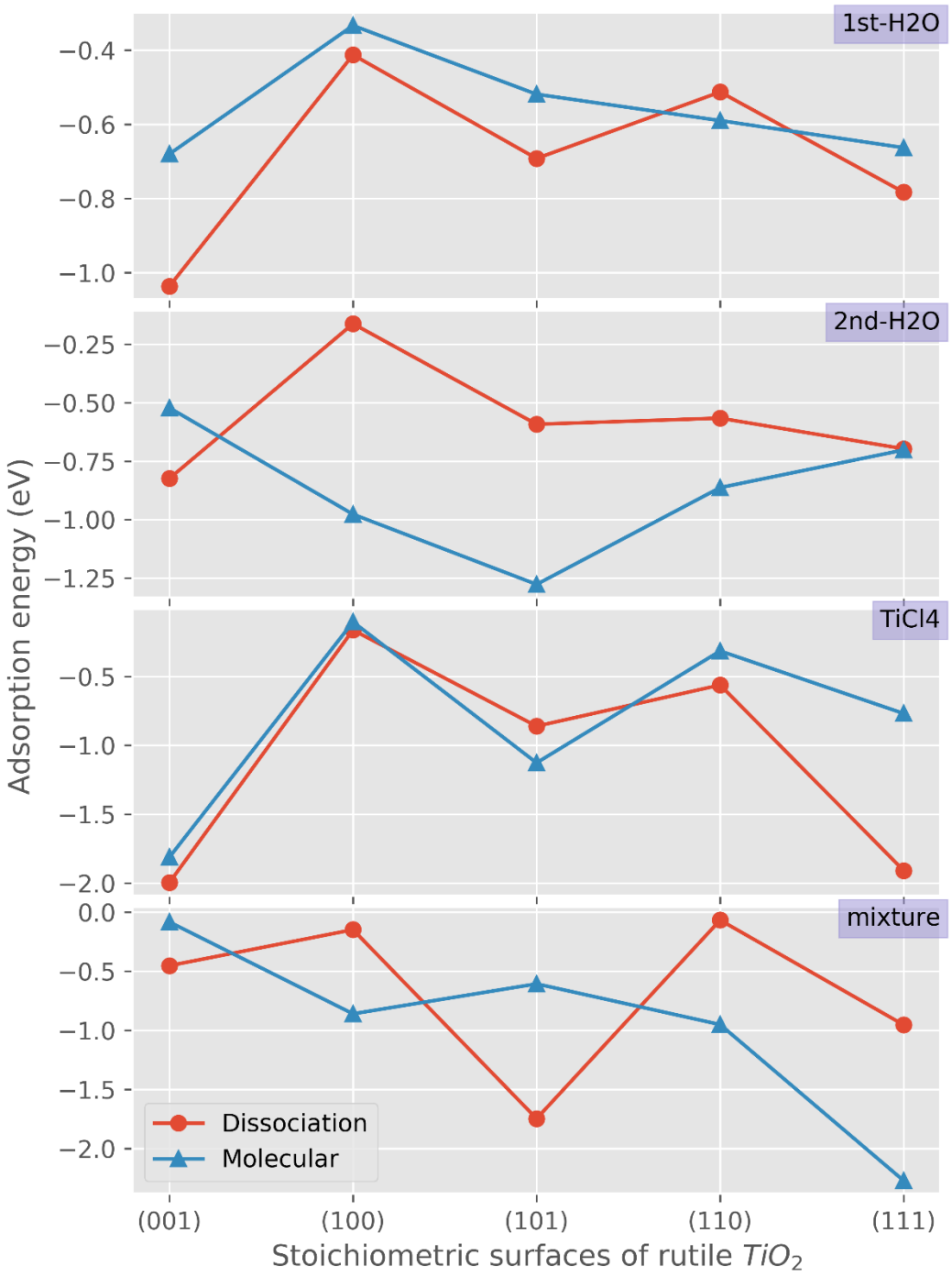

Fig. 3. Adsorption energy of each termination on different stoichiometric surfaces of rutile TiO_2 with different absorbates (i.e., 1^{st}-H_2O, 2^{nd}-H_2O, $TiCl_4$, and the mixture of one water molecule with pre-adsorbed $TiCl_4$). The more negative adsorption energy, the more stable adsorption which is equivalent to adsorption preference.

3.3. Adsorption of $TiCl_4$

We consider the molecular and dissociative adsorption of $TiCl_4$ as schematized in Figure 4. Table 3 and Figure 3 summarize the adsorption energies obtained, Table S2 displays the optimized structures. Two molecular structures have been explored, “molecular-Ti” where the molecule binds through the Ti atom to a surface oxygen (distorting the molecule), and “molecular-Cl” where it binds through a Cl atom. The adsorption energy is calculated in the same way as the first water adsorption, equation 2. Figure 4 shows the adsorption energy difference between those two structures. The molecular-Ti mode is preferred over the molecular-Cl mode for all the terminations, with energies ranging from -1.81 eV (001) to -0.10 eV (100). It can be observed in Figure 4 that the molecular-Ti mode makes four bonds with the surface, whereas the molecular-Cl only one. However the dissociative mode is found to be more exothermic and reached -1.99 eV for the (001) and -1.91 eV for the (111) terminations. With the exception of the (101) termination, dissociation is more favorable than molecular adsorption. The (001) and (111) slabs display the most negative values and lead to the doubly dissociated $TiCl_2$/2Cl mode, whereas the (100) and (110) are less negative and lead to $TiCl_3$/Cl modes. The same behavior was observed for the water adsorption: (100) and (111) terminations display the most exothermic values and lead to dissociation.

It is worth noting that $TiCl_4$ adsorbs more strongly than water on the (001), (111) and (101) and thus would displace adsorbed water from the surface (see Table 4). On the contrary, water adsorbs more strongly than $TiCl_4$ on (100) and (110) and would thus not displace water, making the growth impossible due to the lack of Ti source. The ability to dissociate $TiCl_4$ is therefore also a key point since the growth of TiO_2 needs to break Ti-Cl bonds and create Ti-O bonds. This seems to be better achieved in (001) and (111) terminations where two Ti-Cl bonds are broken with energies close to -2 eV; the (110) termination presents similar values for $TiCl_3$/Cl and $TiCl_2$/2Cl but less exothermic adsorption energy -0.56 eV and -0.52 eV, respectively, making this termination less attractive for the precursor.

Table 3. Adsorption energies in eV for molecular and dissociated $TiCl_4$ on the five terminations.

Surface	Molecular		Dissociative	
	-Ti	-Cl	$TiCl_3$/Cl	$TiCl_2$/2Cl
(001)	-1.81	0.00	-1.85	-1.99
(100)	-0.10	0.12	-0.16	-0.15
(101)	-1.13	-0.01	-0.83	-0.86
(110)	-0.31	0.05	-0.56	-0.52
(111)	-0.77	-0.06	-1.82	-1.91

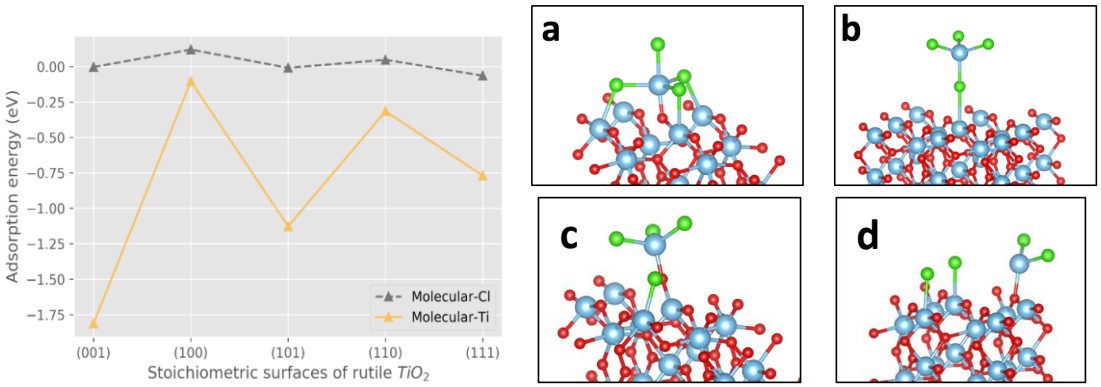

Fig. 4. Left, adsorption energy of molecular $TiCl_4$ for each termination. Right, geometry of a) molecular-Ti b) molecular-Cl c) dissociative $TiCl_3$/Cl d) dissociative $TiCl_2$/2Cl (chlorine atoms in green, Ti in light blue and O in red).

3.4. Coadsorption of water and $TiCl_4$

The results presented above point to a key role of the adsorption of $TiCl_4$ as a source of Ti atoms that would displace water and stabilize the (001) and (111) terminations. In order to establish the affinity of water in the presence of precursor we have computed the coadsorption of the two molecules on the titania slab models. This situation ressembles more the actual hydrothermal synthesis experiment in which solvent and precursor are introduced simultaneously in the autoclave. Our starting point is the optimized $TiCl_4$ system for each termination, on top of which we adsorb a

water molecule. This picture is coherent for the (001) and (111) terminations for which $TiCl_4$ would clearly displace water, and (101) which exhibits similar affinity for water and $TiCl_4$. We have included also (100) and (110) terminations for the sake of comparison.

Table 4 summarizes the results obtained for the five terminations as regards separate adsorptions and coadsorption, and Figure 5 displays the optimized geometry for the (001) and (111) terminations. The (001) termination containing $TiCl_4$ would adsorb water dissociatively by -0.45 eV. Interestingly, the $TiCl_3$ moiety binds to a hydroxyl group connected to the surface. The topology of the surface makes that the surface OH group is close to the $TiCl_3$ unit. A Ti-Cl species is thus formed, similar to that corresponding to atomic chlorine on metal oxides[13]. The (111) termination would adsorb water molecularly with -2.27 eV. The optimized geometry is presented in Figure 5 and it can be observed that the $TiCl_3$ unit is only bonded to the surface, whereas a Cl atom binds to two surface Ti sites. In view of an atomic mechanism where Ti-Cl and O-H bonds break, and Ti-O bonds form, the (001) termination seems to provide the most plausible scenario according to our results. The (101) termination would also favor water dissociation in the neighborhood of $TiCl_4$ by -1.74 eV, but considering that $TiCl_4$ would preferentially go to (001) or (111) terminations this process would not be favored. The (100) and (110) terminations also display the same behavior as (101) but the affinity of $TiCl_4$ is not energetically favored and thus not expected.

Table 4. Adsorption energy in eV for the separate adsorbates: precursor $TiCl_4$ on a bare slab, one water molecule on a bare slab (1^{st}-H_2O), a second water molecule on the bare slab (2^{nd}-H_2O) and a water molecule on a $TiCl_4$-containing slab (coadsorption). *d* stands for dissociative and *m* for molecular adsorption.

Surface	$TiCl_4$	1^{st}-H_2O	2^{nd} H_2O	H_2O on $TiCl_4$-substrate	
				molecular	dissociative
(001)	-1.99 d	-1.03 d	-0.82 d	-0.08	-0.45
(100)	-0.16 d	-0.41 d	-0.98 m	-0.86	-0.15
(101)	-1.13 m	-0.69 d	-1.28 m	-0.61	-1.74
(110)	-0.56 d	-0.59 m	-0.86 m	-0.95	-0.07
(111)	-1.91 d	-0.78 d	-0.70 d	-2.27	-0.95

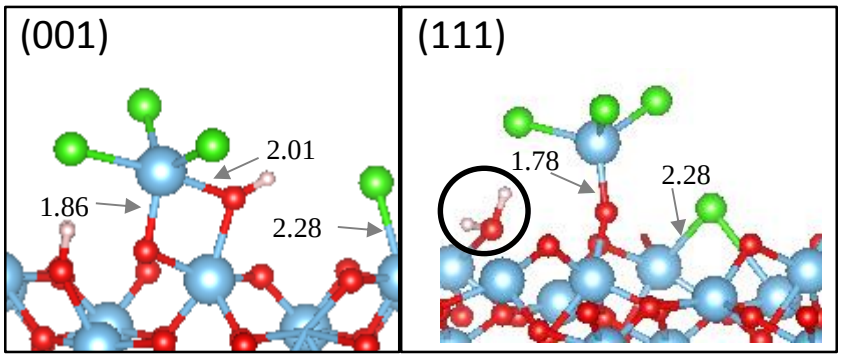

Figure 5. Selected views of the optimized co-adsorption models of $TiCl_4$ and water on (001) and (111) terminations. Distances in Å.

4. Discussion

The first step to propose a mechanism for the growth mechanism on rutile TiO_2 substrates is to analyze the interaction energy of the precursors with the stoichiometric terminations. As regards the strength, the Ti-precursor $TiCl_4$ is found to adsorb strongly compared to the O-precursor, water. Considering that water is in large excess, the growth will be limited by the adsorption of $TiCl_4$ that would displace water from the surface. Interestingly, our results indicate that $TiCl_4$ will stabilize on (100) and (111) terminations strongly, -1.99 eV and -1.91 eV respectively. Such preferential adsorption can explain the growth of rutile nanorods in the (001) direction. This mechanism has been used in the literature to explain the synthesis of Pt nanocubes in the presence of H_2 that adsorbs more strongly on (100) facets [14].

The second factor to consider is the need of making Ti and O available to form Ti-O bonds. This involves in our study that Ti-Cl bonds in $TiCl_4$ should be broken, as well as O-H in water, and thus dissociative modes should play a key role. Our results support that $TiCl_4$ dissociates on the (001) and (111) slab models leading to $TiCl_2$/2Cl and $TiCl_3$/Cl surface species. In addition, the adsorption of a water molecule on this system (coadsorption) is energetically favorable by -0.45 eV, and is dissociative i.e. forms surface hydroxyl groups. From this perspective, both (001) and (111) terminations seem to be good candidates.

Finally, the formation of Ti-O new bonds should be favored. This can be achieved by an appropriate local topology. For the (001) model it was found that optimization

of the coadsorption structure led to the formation of a new Ti-OH bond: the Ti(Cl_3) atom lies in the vicinity of the hydroxyl group that comes from water dissociation, resulting in a (Cl_2)Ti(OH) moiety (Figure 5). Such fragment could be an important intermediate creating new TiO_2 layers. For comparison, the local topology of (111) termination with $TiCl_3$/Cl species does not provide a favorable local geometry to form adsorbate-adsorbate bonds and is thus less convincing. This points to the (001) termination as an optimal support for the growth of rutile overlayers.

To summarize, the morphology of the different facets of rutile allow pointing to selective interaction with the precursors as a plausible cause for the 1D growth in the (001) direction observed in the experiments. The energetics of the Ti and O sources, the ease in breaking Ti-Cl and O-H bonds and a favorable topology to form new Ti-O bonds is optimal in the (001) models. It is worth noting that other phenomena could be involved in the growth mechanism: presence of other reactants (acid, tinfoil, substrate), conditions (pressure, temperature, time) may influence the dynamics of growth and the nature of the products obtained. In the present study, $TiCl_4$ intermediate seems to play a key role in the mechanism since its interaction with (001) terminations appears to be extremely specific. Its observation has not been reported so far, and its formation might lie at the origin of the nanorods formation. Its absence in the media (for instance by employing a different acid than HCl, or by considering other Ti precursors, such a titanium foil instead of TBOT) might affect significantly the chemical equilibria in the reaction bath and therefore the growth mechanism.

The identification of selective surface-intermediate interactions, such as $TiCl_4$-(001), could provide new insight in the synthesis of size and shape-controlled nanomaterials. We hope to stimulate experimental work to characterize key species and intermediates involved in bottom-up nanoparticle growing processes.

5. Conclusions

In the one-step hydrothermal synthesis experiment[3], 1D mixed phase TiO_2 nanorod array can be synthesized in high quality, large-scale and free-standing film. However little is known about the reactions taking place in the autoclave, hindering the understanding of the process. In the present study we use *ab initio* calculations to model the interaction of Ti and O precursors with five terminations of TiO_2, in order to identify key factors affecting the selective growth in the [001] direction observed experimentally.

Our results show that the Ti-precursor $TiCl_4$ adsorbs strongly and selectively on the (001) termination, resulting in dissociated species that bind to neighboring

hydroxyl groups. Such interaction has only been observed in the (001) termination, and is due to the peculiar topology of the surface.

The present study provides a plausible scenario to explain the growth in a preferential direction on a molecular level. It brings crucial information on the mechanistic aspects that lead precursors to interact on the substrate and create new TiO_2 layers, otherwise inaccessible by the experiment. We hope that our theoretical results will stimulate new experiments to reveal the growth mechanism in TiO_2 and other materials.

Acknowledgements

This work was performed in the Erasmus Mundus + program EURASIACAT 552067-EM-1-2014-1-ES-ERA MUNDUS-EMA22. It was also financially supported by the Environmental Protection Administration of Taiwan, NTU Research Center for Future Earth from The Featured Areas Research Center Program within the framework of the Higher Education Sprout Project by the Ministry of Education of Taiwan, and Ministry of Science and Technology of Taiwan. The authors acknowledge Scienomics for the MAPS program used in the construction of the slab models for a courtesy license. Dr. B. Diawara is acknowledged for the Modelview program. This work was performed using HPC resources from GENCI-CINES/IDRIS (Grant 2018- x2018082131 and 2019- x2019082131).

References

1. (a) Chen, Y.; Tao, Q.; Fu, W.; Yang, H.; Zhou, X.; Su, S.; Ding, D.; Mu, Y.; Li, X.; Li, M., Enhanced photoelectric performance of PbS/CdS quantum dot co-sensitized solar cells via hydrogenated TiO_2 nanorod arrays. *Chemical Communications* **2014,** *50* (67), 9509-9512; (b) Hou, Y.; Li, X.; Zou, X.; Quan, X.; Chen, G., Photoeletrocatalytic Activity of a Cu_2O-Loaded Self-Organized Highly Oriented TiO_2 Nanotube Array Electrode for 4-Chlorophenol Degradation. *Environmental Science & Technology* **2009,** *43* (3), 858-863; (c) Liu, B.; Chen, H. M.; Liu, C.; Andrews, S. C.; Hahn, C.; Yang, P., Large-Scale Synthesis of Transition-Metal-Doped TiO_2 Nanowires with Controllable Overpotential. *Journal of the American Chemical Society* **2013,** *135* (27), 9995-9998; (d) Nguyen, N. T.; Yoo, J.; Altomare, M.; Schmuki, P., "Suspended" Pt nanoparticles over TiO_2 nanotubes for enhanced photocatalytic H2 evolution. *Chemical Communications* **2014,** *50* (68), 9653-9656; (e) Zhu, K.; Neale, N. R.; Miedaner, A.; Frank, A. J., Enhanced Charge-Collection Efficiencies and Light Scattering in Dye-Sensitized Solar Cells Using Oriented TiO2 Nanotubes Arrays. *Nano Letters* **2007,** *7* (1), 69-74; (f) Frank, A. J.; Kopidakis, N.; van de Lagemaat, J., *Electrons in nanostructured TiO_2 solar cells: Transport, recombination and photovoltaic properties*. 2004; Vol. 248, p 1165-1179.

2. (a) Cong, S.; Xu, Y., Explaining the High Photocatalytic Activity of a Mixed Phase TiO_2: A Combined Effect of O_2 and Crystallinity. *The Journal of Physical Chemistry C* **2011,** *115* (43), 21161-21168; (b) Henderson, M. A., A surface science perspective on TiO2 photocatalysis. *Surface Science Reports* **2011,** *66* (6), 185-297; (c) Hurum, D. C.; Gray, K. A.; Rajh, T.; Thurnauer, M. C., Recombination Pathways in the Degussa P25 Formulation of TiO_2: Surface versus Lattice Mechanisms. *The Journal of Physical Chemistry B* **2005,** *109* (2), 977-980; (d) Scanlon, D. O.; Dunnill, C. W.; Buckeridge, J.; Shevlin, S. A.; Logsdail, A. J.; Woodley, S. M.; Catlow, C. R. A.; Powell, M. J.; Palgrave, R. G.; Parkin, I. P.; Watson, G. W.; Keal, T. W.; Sherwood, P.; Walsh, A.; Sokol, A. A., Band alignment of rutile and anatase TiO_2. *Nature Materials* **2013,** *12*, 798.

3. Kao, L. C.; Lin, C. J.; Dong, C. L.; Chen, C. L.; Liou, S. Y. H., Transparent free-standing film of 1-D rutile/anatase TiO_2 nanorod arrays by a one-step hydrothermal process. *Chemical Communications* **2015,** *51* (29), 6361-6364.

4. (a) Fox, H.; Newman, K. E.; Schneider, W. F.; Corcelli, S. A., Bulk and Surface Properties of Rutile TiO_2 from Self-Consistent-Charge Density Functional Tight Binding. *Journal of Chemical Theory and Computation* **2010,** *6* (2), 499-507; (b) Helali, Z.; Jedidi, A.; Syzgantseva, O. A.; Calatayud, M.; Minot, C., Scaling

reducibility of metal oxides. *Theoretical Chemistry Accounts* **2017,** *136* (9), 100.
5. (a) Di Valentin, C.; Pacchioni, G.; Selloni, A., Electronic Structure of Defect States in Hydroxylated and Reduced Rutile TiO_2(110) Surfaces. *Phys. Rev. Lett.* **2006,** *97*, 166803; (b) Labat, F.; Baranek, P.; Adamo, C., Structural and Electronic Properties of Selected Rutile and Anatase TiO2 Surfaces: An ab Initio Investigation. *Journal of Chemical Theory and Computation* **2008,** *4* (2), 341-352; (c) Bouzoubaa, A.; Markovits, A.; Calatayud, M.; Minot, C., Comparison of the reduction of metal oxide surfaces: TiO2-anatase, TiO2-rutile and SnO2-rutile. *Surf. Sci.* **2005,** *583*, 107-117; (d) Perron, H.; Domain, C.; Roques, J.; Drot, R.; Simoni, E.; Catalette, H., Optimisation of accurate rutile TiO_2 (110), (100), (101) and (001) surface models from periodic DFT calculations. *Theoretical Chemistry Accounts* **2007,** *117* (4), 565-574.
6. (a) Chen, X.; Selloni, A., Introduction: Titanium Dioxide (TiO_2) Nanomaterials. *Chemical Reviews* **2014,** *114* (19), 9281-9282; (b) De Angelis, F.; Di Valentin, C.; Fantacci, S.; Vittadini, A.; Selloni, A., Theoretical Studies on Anatase and Less Common TiO_2 Phases: Bulk, Surfaces, and Nanomaterials. *Chemical Reviews* **2014,** *114* (19), 9708-9753; (c) Ko, K. C.; Lee, J. Y.; Illas, F., Chapter 7 - Modeling realistic titania nanoparticles. In *Frontiers of Nanoscience*, Bromley, S. T.; Woodley, S. M., Eds. Elsevier: 2018; Vol. 12, pp 205-238; (d) Nunzi, F.; Agrawal, S.; Selloni, A.; Angelis, F. D., Structural and Electronic Properties of Photoexcited TiO_2 Nanoparticles from First Principles. *Journal of Chemical Theory and Computation* **2015,** *11* (2), 635-645.
7. (a) Qu, Z.-w.; Kroes, G.-J., Theoretical Study of Stable, Defect-Free (TiO2)n Nanoparticles with n = 10-16. *The Journal of Physical Chemistry C* **2007,** *111* (45), 16808-16817; (b) Hamad, S.; Catlow, C. R. A.; Woodley, S. M.; Lago, S.; Mejias, J. A., Structure and Stability of Small TiO_2 Nanoparticles. *The Journal of Physical Chemistry B* **2005,** *109* (33), 15741-15748; (c) Berardo, E.; Hu, H.-S.; Shevlin, S. A.; Woodley, S. M.; Kowalski, K.; Zwijnenburg, M. A., Modeling Excited States in TiO_2 Nanoparticles: On the Accuracy of a TD-DFT Based Description. *Journal of Chemical Theory and Computation* **2014,** *10* (3), 1189-1199; (d) Calatayud, M.; Minot, C., Is There a Nanosize for the Activity of TiO_2 Compounds? *Journal of Physical Chemistry C* **2009,** *113* (28), 12186-12194; (e) Syzgantseva, O. A.; Gonzalez-Navarrete, P.; Calatayud, M.; Bromley, S.; Minot, C., Theoretical Investigation of the Hydrogenation of $(TiO_2)_N$ Clusters (N = 1–10). *The Journal of Physical Chemistry C* **2011,** *115* (32), 15890-15899.
8. (a) Kresse, G.; Furthmüller, J., Efficient iterative schemes for ab initio total-energy calculations using a plane-wave basis set. *Phys. Rev. B* **1996,** *54* (16), 11169-11186; (b) Kresse, G.; Furthmüller, J., Efficiency of ab-initio total energy

calculations for metals and semiconductors using a plane-wave basis set. *Computational Materials Science* **1996,** *6* (1), 15-50; (c) Kresse, G.; Hafner, J., Ab initio molecular dynamics for liquid metals. *Physical Review B* **1993,** *47* (1), 558-561; (d) Kresse, G.; Hafner, J., Ab initio molecular-dynamics simulation of the liquid-metal--amorphous-semiconductor transition in germanium. *Physical Review B* **1994,** *49* (20), 14251-14269.
9. Perdew, J. P.; Burke, K.; Ernzerhof, M., Generalized Gradient Approximation Made Simple. *Physical Review Letters* **1996,** *77* (18), 3865-3868.
10. Blochl, P. E., Projector augmented-wave method. *Phys. Rev. B* **1994,** *50*, 17953-17979.
11. Hardcastle, T.; M D Brydson, R.; Livi, K.; R Seabourne, C.; J Scott, A., *Ab-initio modelling, polarity and energetics of clean rutile surfaces in vacuum and comparison with water environment*. 2012; Vol. 371.
12. (a) Sun, C.; Liu, L.-M.; Selloni, A.; C Smith, S., *Titania-water interactions: A review of theoretical studies*. 2010; Vol. 20; (b) Liu, L.-M.; Zhang, C.; Thornton, G.; Michaelides, A., Structure and dynamics of liquid water on rutile TiO_2 (110). *Physical Review B* **2010,** *82* (16), 161415; (c) Cuko, A.; Macià Escatllar, A.; Calatayud, M.; Bromley, S. T., Properties of hydrated TiO_2 and SiO_2 nanoclusters: dependence on size, temperature and water vapour pressure. *Nanoscale* **2018,** *10* (45), 21518-21532; (d) Di Valentin, C.; Tilocca, A.; Selloni, A.; Beck, T. J.; Klust, A.; Batzill, M.; Losovyj, Y.; Diebold, U., Adsorption of Water on Reconstructed Rutile TiO_2(011)-(2×1): TiO Double Bonds and Surface Reactivity. *Journal of the American Chemical Society* **2005,** *127* (27), 9895-9903; (e) Vittadini, A.; Selloni, A.; Rotzinger, F. P.; Grätzel, M., Structure and energetics of water adsorbed at TiO_2 anatase (101) and (001) surfaces. *Phys. Rev. Lett.* **1998,** *81*, 2954-2957; (f) Li, W.-K.; Gong, X.-Q.; Lu, G.; Selloni, A., Different Reactivities of TiO_2 Polymorphs: Comparative DFT Calculations of Water and Formic Acid Adsorption at Anatase and Brookite TiO2 Surfaces. *The Journal of Physical Chemistry C* **2008,** *112* (17), 6594-6596; (g) Kavathekar, R. S.; Dev, P.; English, N. J.; MacElroy, J. M. D., Molecular dynamics study of water in contact with the TiO2 rutile-110, 100, 101, 001 and anatase-101, 001 surface *Molecular Physics* **2011,** *109* (13), 1649-1656.
13. Calatayud, M.; Markovits, A.; Menetrey, M.; Mguig, B.; Minot, C., Adsorption on perfect and reduced surfaces of metal oxides. *Catalysis Today* **2003,** *85* (2-4), 125-143.
14. Aguilera-Porta, N.; Calatayud, M.; Salzemann, C.; Petit, C., Understanding How in Situ Generated Hydrogen Controls the Morphology of Platinum Nanoparticles. *The Journal of Physical Chemistry C* **2014,** *118* (17), 9290-9298.